International Journal of Engineering and Information Systems (IJEAIS)
ISSN: 2000-000X
Vol. 1 Issue 7, September – 2017, Pages: 104-112

A Narrow Band BPF for UWB RFID Reader Circuit for Frequency Extraction

A.K.M Zakir Hossain, M. I. Ibrahimy* and S. M. A. Motakabber
Department of Electrical and Computer Engineering
International Islamic University Malaysia
Kuala Lumpur, Malaysia
*Corresponding Author's Email: ibrahimy@iium.edu.my

***Abstract**: In this article, a narrow band, open circuited planar microstrip band pass filter has been proposed. Existing RFID reader circuits has to generate a constant chirp signal to read the conventional microstrip resonator type tag. Use of the VCO is well established for this application. However, in case of large bandwidth (≥ 4GHz) chirp generation it's still challenging for the researchers. This problem can be mitigated by using as many numbers of mixer-filter combinations as needed. Successful implementation of this topology centres around the precise design of a very narrow (<2% fractional bandwidth) band BPF. The proposed structure has been designed, simulated and fabricated for 5.4GHz. It is observed that the fractional bandwidth of the BPF is less than 2% of the center frequency. The simulation and measured S-Parameters are in good agreement. The final bandwidth of the designed filter is 100MHz and the dimensions24.3 mm X 5 mm.*

Keywords— Planar microstrip; RFID; VCO; BPF; fractional bandwidth

1. INTRODUCTION

Since the invention and application of the Radio Frequency Identification (RFID) in World War II for the purpose to distinguish between the friend and foe, this technology has come a long way. Nowadays, RFID is getting a huge attention because of its many advantages over the traditional bar code system (no need of line of sight (LOS) connection, low risk of atmospheric effects, less sensitivity to wear and tear etc. [1]. This technology has many applications (especially in automation) in diverse industries such as item tracking, toll collection, data entry in the range of the inventory management and logistics system to agriculture and food. However, the sectors such as library managements where it involves the large scale item tagging the optical barcodes still has the dominancy over the RFID [2].

RFID systems can be classified in many ways. On the basis of its frequency of operation it is low frequency (125 KHz), high frequency (13.56MHz), ultra high frequency (860 to 930 MHz), microwave (2.45 GHz) and ultra wide band (UWB) that working between 3.1 to 10.7 GHz. In each working band of frequencies different detection techniques and topologies are adopted while designing the system. Moreover, the dimensions of the tag are also a function of the operating frequency [3, 4].

Similarly, on the basis of on board tag power supply it is classified as, active type tag that relies of its transmission, reception and other functions on the battery on-board, semi-active type tag that also has battery on board only to keep the digital circuitry alive but needs the assistance of reader interrogation signal power to send and receive the information and passive type tag which comprises no battery on board and totally dependent on the interrogation signal power to perform all necessary operations. The chipless type tags don't carry any silicon chip on-board so it is inherently passive in nature [5]. Since there is no inclusion of chip on board the chipless tag is the main competitor to replace the conventional barcode system.

Nowadays, a number of active and passive RFID systems in different frequencies are available in the market. Hence, a wide range of RFID tag and their corresponding reader are available in the commercial market [6]. At present, chipless RFID technology opens a new research area in RFID due to its simplicity and low cost since a chipless tag doesn't hold any silicon chip and no classical RF modulation schemes are required for communication [7]. The UWB enables a wide frequency range for the researchers to design different chipless RFID systems and UWB RFID systems are now at the forefront of the of the research. However, the UWB RFID technology is not omnipresent and yet to be fully deployed commercially [3].

Recently, the chipless RFID reader approaches are complex, bulky, expensive and commercially inadequate in the market. Their existences are still in the incubation stages inside the research lab [8]. Though the chipless tag price is going lower, however the price of the reader is still very high and the dimension of reader is also bulky. As a result, these are the big issues at present to the RFID end users. An UWB RFID reader is an RF transceiver. This actually makes the system bulky, costly and complex. One of the

solutions is to use the RF switch but, in this case implementation of the switch cannot be feasible because the reader keeps sending the CW signal while receiving the backscatter signal from the tag. Also because of the large bandwidth of the UWB system the generation of the constant analogue chip signal is very difficult and difficult to find and also expensive in the existing market. This makes a conclusion that one reader can be made in such a way that there is no constant chirp but only the corresponding signals related to the tag. Fig. 1 shows the topology of the reader front-end for frequency extraction [9].

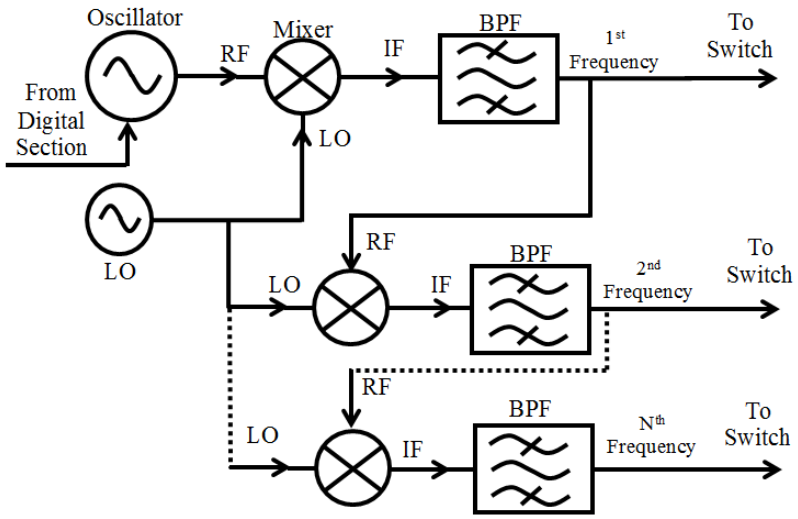

Fig. 1. *Frequency extraction RFID reader front-end topology.*

It is well known from the theory of mixer that the RF mixer takes two different signals as input (radio frequency and local oscillator signal), multiplies them and produces a large amount of different signals. Therefore, a sharp narrow band higher order band pass filter (BPF) is essential to extract a particular frequency from all of the produced frequencies from the mixer. Recently in [9] the authors have proposed a topology to extract the desired frequency for RFID reader interrogation signal in UWB region for passive tags. The BPF's bandwidth has to be narrow enough to extract the generated desired frequency among them which depends on the quality of the design. The adopted topology is coupled line BPF [10] and the structure is shown in Fig. 2.

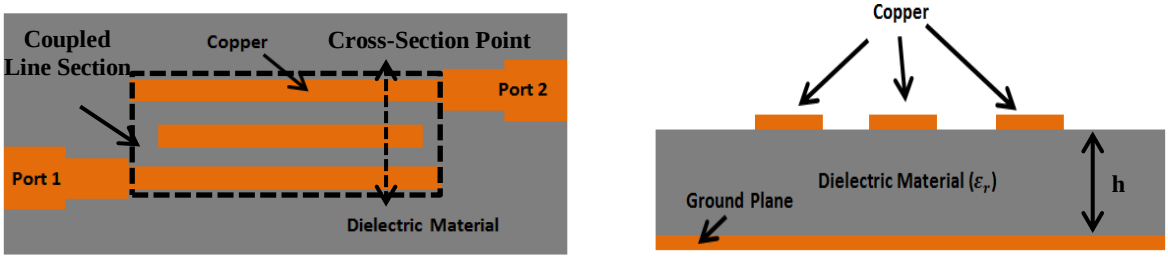

(a) Top View (b) Cross-sectional View

Fig. 2. *The filter structure (a) top view and (b) cross-sectional view.*

2. Filter Structure and Design

Narrowband band pass filters can be made with parallel coupled line sections of the form shown in Fig. 2. Shown in Fig. 2(a) is the top view of the filter geometry where the coupled line patches are on the same plane. There are three parallel coupled microstrip lines on the top of the PCB. The outer two lines have same length but line in between them has different length then them. Tapered line is used for both input and output port of the filter. By changing the length of the middle conductor gives the freedom of tuning the filter for different frequencies at a time. Fig. 2(b) illustrates the cross-sectional view of the proposed structure. Usually, the coupled lines filter shows less and about 20% of the bandwidth of its center frequency. In this project the necessity is to make a filter as narrow as less than 1% of the center frequency. From the theory of the coupled line the impedances (even and odd mode) are approximated. The process follows the equations (1) and (2) respectively [10].

$$Z_{ine} = \lim_{Z_L \to \infty} Z_{0e} \frac{Z_L + jZ_{0e}tan\theta_e}{Z_{0e} + jZ_L tan\theta_e} \quad (1)$$

$$Z_{ino} = \lim_{Z_L \to \infty} Z_{0o} \frac{Z_L + jZ_{0o}tan\theta_e}{Z_{0o} + jZ_L tan\theta_e} \quad (2)$$

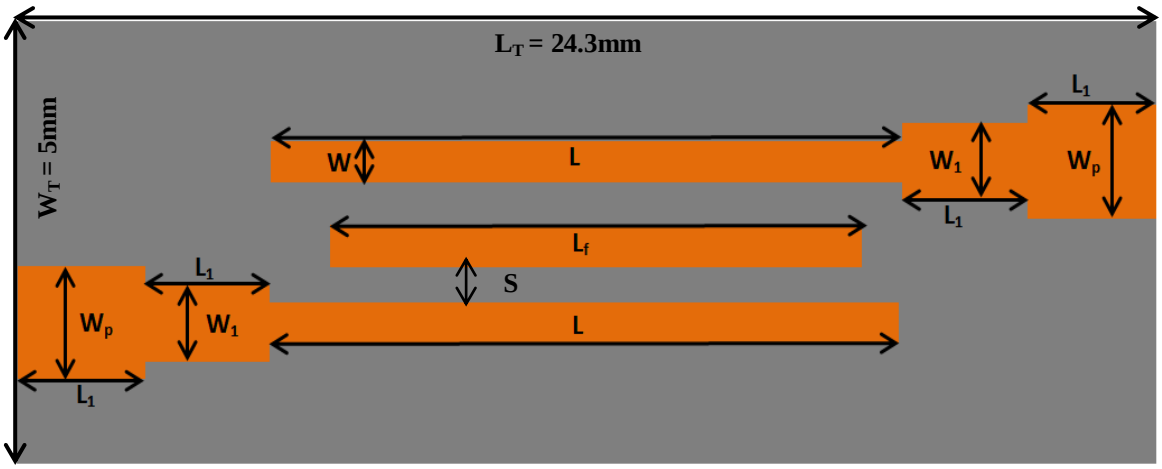

Fig. 3. *Structure of the BPF and parameters.*

Where, Z_{0e} and Z_{0o} are the even and odd mode characteristic impedances of the coupled lines respectively, θ_e and θ_o are the electrical lengths for even- and odd-mode excitations, respectively. The condition for the reflection zero, namely $S_{11}= 0$, is $Z_{ine} = Z_{ino}$. As $Z_L = \infty$ (open circuited), the condition for obtaining the location of reflection zeros of the open circuited parallel-coupled lines is given by equation (3),

$$\frac{Z_{0e}}{Z_{0o}} = \frac{cot\theta_e}{cot\theta_o} \quad (3)$$

For obtaining the good narrow pass-band performance of the proposed filter, the electrical length of the microstrip parallel-coupled lines with short-circuit is equivalent to quarter-wavelength since the structure can exhibit all-pass response with multiple reflection zeros. Fig. 3 shows the parametric view of the proposed structure. The optimized parameters are listed in Table 1. In the design, the proposed filter is implemented on the Taconic TLX-8 with a dielectric constant of $\varepsilon_r = 2.55$, a loss tangent of 0.0019, and a thickness h of 0.5 mm. The input/output ports are all designed for 50Ω. The structure is simulated optimized in CST MWS 2016 [11]. Fig. 4 shows the filter structure in CST MWS environment.

Table 1. List of parameters

Parameters	Unit (mm)
W	0.4
W_p	1.41
W_1	0.8
S	0.4
L	14.3
L_1	2.5
L_f	11

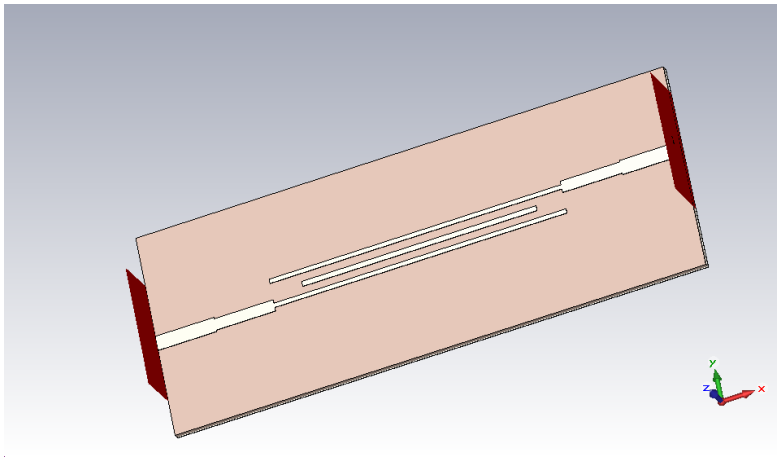

Fig. 4. *The modeled filter geometry in CST MWS*

When the circuit parameters are L = 14.3 mm, W = 0.4 mm, L_f = 11 mm, W_p = 1.4mm and W_1 = 0.8mm as shown in Fig. 3, the characteristic impedances Z_{0e} and Z_{0o} of the open circuited parallel-coupled line with quarter-wavelength at 5.4 GHz are calculated to be 159.73Ω and 90.01Ω, respectively.

3. EM Simulation and Experiential Results

Fig. 5(a) and (b) shows the frequency vs S-parameter response both in magnitude and phase of the designed filter structure. Both of the figures have S_{21} and S_{11} responses for the designed filter. It is clearly observed that the resonance point of this filter is 5.43GHz with a -2.3dB insertion loss from the simulation.

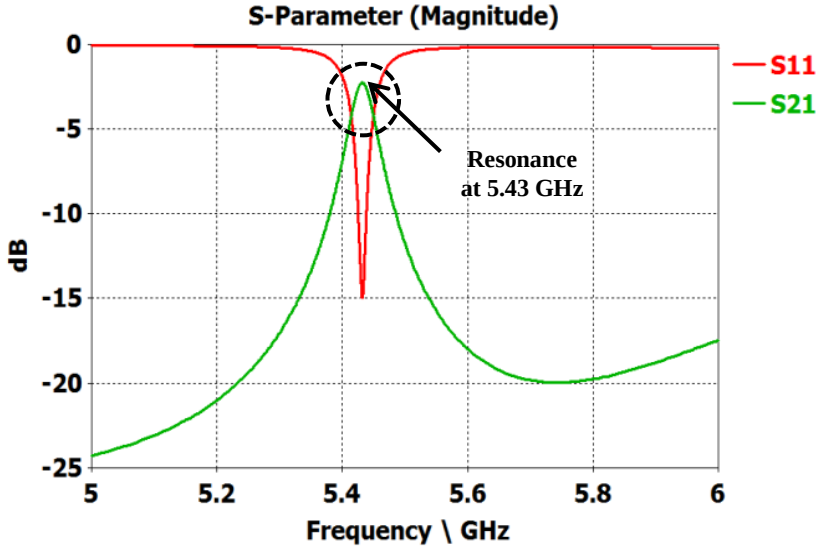

(a) S-parameters Magnitude

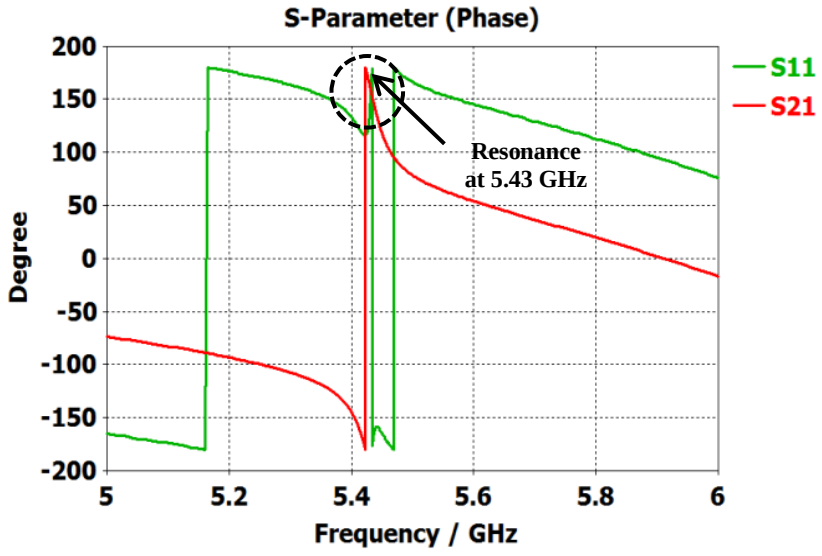

(b) S-parameters Phase

Fig. 5. *S-Parameter responses, (a) Magnitude and (b) Phase.*

Moreover, from S_{11} it is seen that the -10dB bandwidth (BW) around 13MHz and from S21, the -3dB BW is 47MHz. Fig. 6(a), (b) and (c) reveals the simulated surface current of the proposed structure for three different frequencies (4GHz, 5.43GHz and 7GHz respectively). At the frequency of 5.43GHz, the surface current density is high (1127 A/m2) compared to other two non-resonant frequencies (4 GHz and 7 GHz). At 4 GHz and 7 GHz the surface current densities are 261 A/m2 and 393 A/m2 respectively. Figure 6(d) also describes the same scenario. From those figures, it is also justified that the filter has resonance frequency at 5.43GHz.

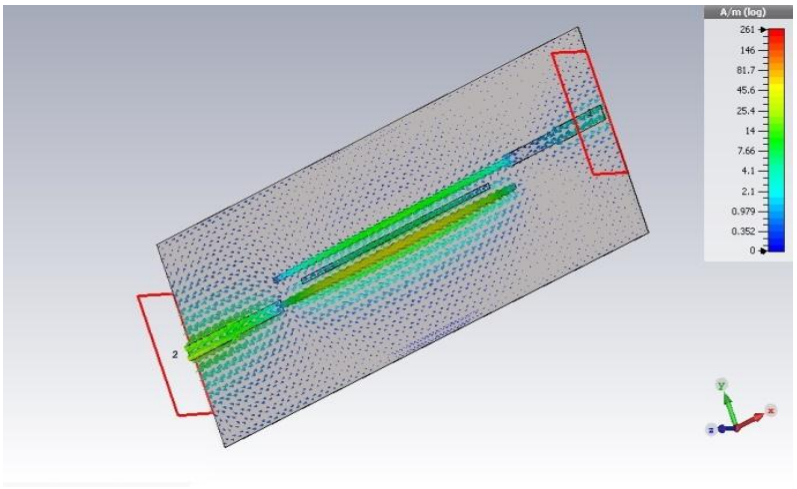

(a) Surface Current (4GHz)

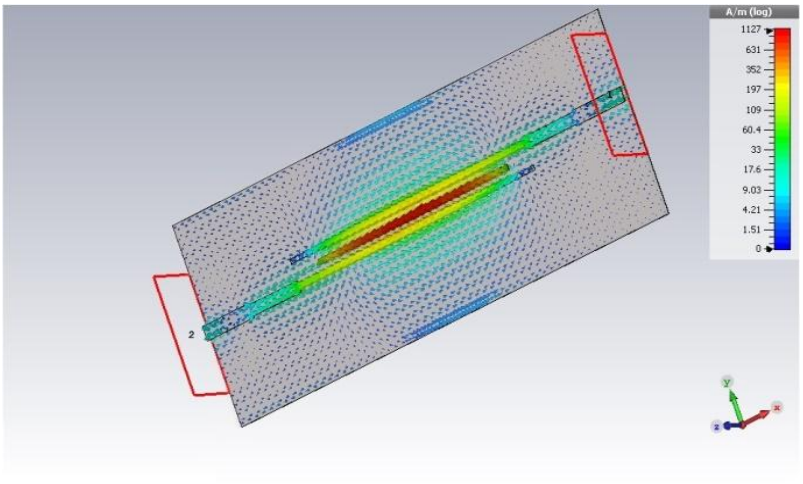

(b) Surface Current (5.43GHz)

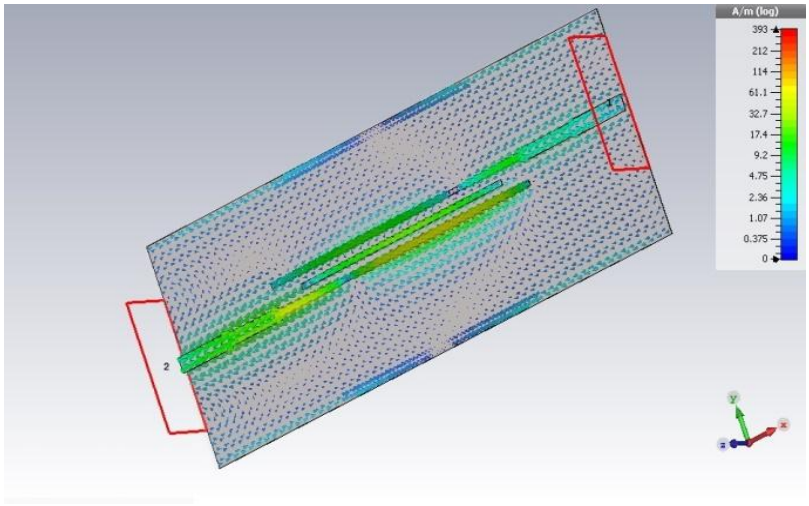

(c) Surface Current (7GHz)

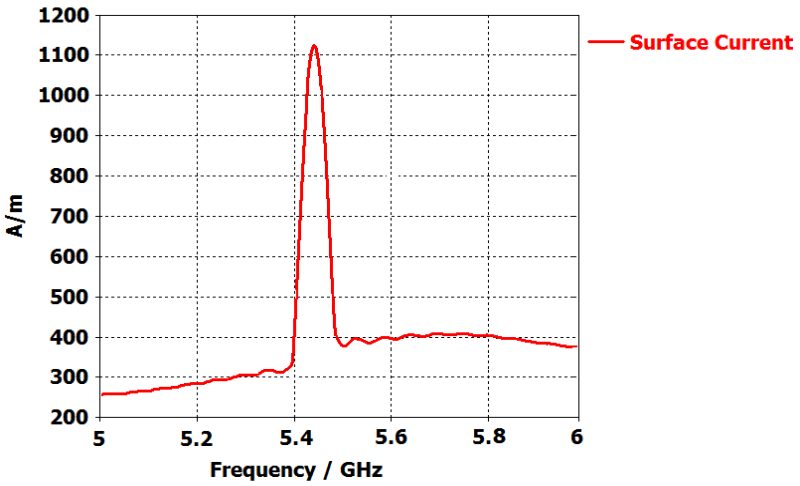

(d) Surface Current Vs frequency

Fig. 6. *The simulated surface current response of the proposed structure.*

After the justification on resonance of the filter structure a parametric sweep has been done by changing the middle conductor length (L_f) from 14.1mm to 14.5mm with a step of 0.1mm. The result is shown in Fig. 7.

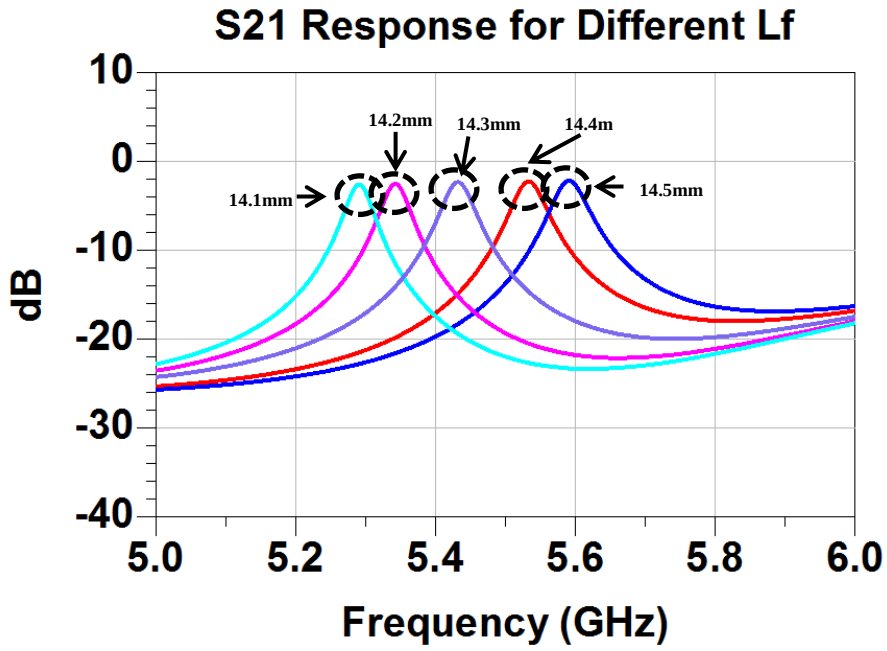

Fig. 7. *Parametric study for different length of L_f*

From Fig. 7, it can be seen that as the length the middle line length (L_f) decreases the resonant frequency increases and vice versa. So it can be concluded that if needed, filters with different resonant frequency can be designed without changing the shape geometry of the filter. Simply with altering the length L_f, the resonant frequency can be tuned.

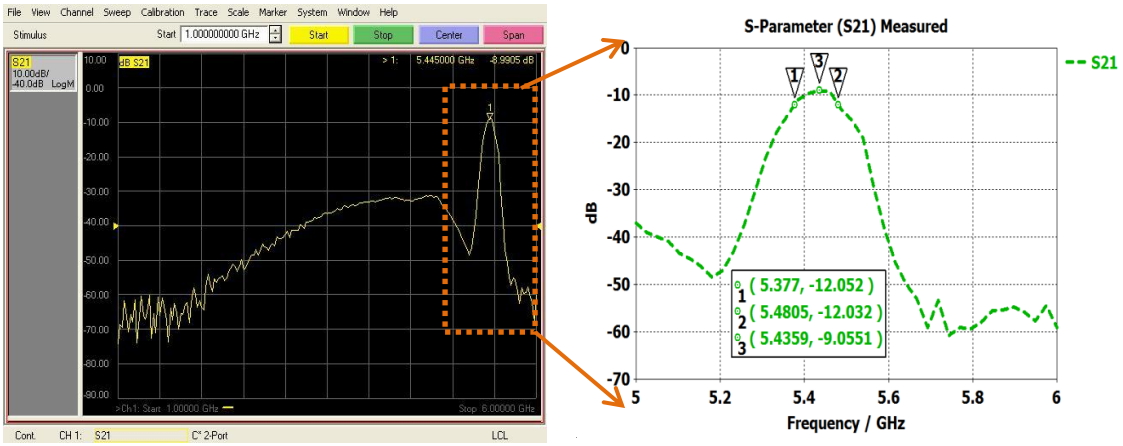

(a) VNA response1GHz to 6GHz

(b) VNA response from 5GHz to 6GHz

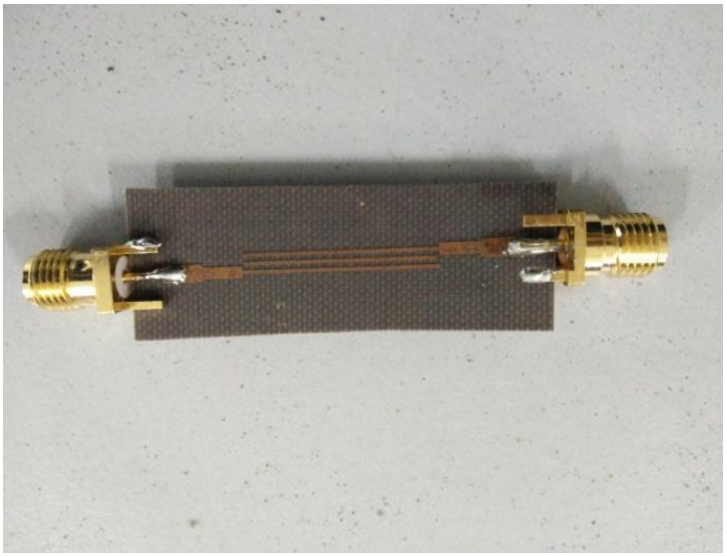

(c) Fabricated filter prototype

Fig. 8. *(a) & (b) VNA responses of the proposed filter and (c) the filter prototype.*

Fig. 8 discloses the fabricated prototype (Fig. 8c) of the proposed filter and its measured S21 response (Fig. 8a and b). The results show that there is a little deviation of resonance point. The insertion loss also deviates from the simulation results. The fabricated prototype gives a resonance frequency of 5.44GHz which have still a close agreement with the simulation. The insertion loss obtained -9.055dB which is much lower than the simulation (-2.3dB). This is may be due to the quality of the fabrication process. Fig. 8(a) illustrates the S21 response of the prototype from 1GHz to 6GHz. To make a better view and understanding of the obtained BW, the VNA data has been imported and plotted in MATLAB 2015b from 5GHz to 6GHz and shown in Fig. 8(b). It can be seen from Fig. 8(b) that the BW obtained after manufacturing the prototype is approximately 100MHz which makes the fractional BW of less than 2% of the resonance frequency (5.43GHz).

4. CONCLUSIONS

A simple open circuited parallel coupled line filter has been designed, simulated, fabricated and measured. The simulated and measured responses are well in agreement. A parametric study has also been made on the middle parallel line length Lf to see the effect of frequency shift of the filter. It is seen from the results that the 3dB BW obtained is 100MHz and the insertion loss is -

9.055dB. The obtained BW is less than 2% of the resonant frequency and can easily be used for the frequency extraction for the UWB RFID reader.

5. ACKNOWLEDGMENT

This research has been supported by the Malaysian Ministry of Science and Technology through the eScienceFund under the project ID: SF14-010-0060.

6. REFERENCES

[1] Nambiar, A. N. (2009, October). RFID technology: A review of its applications. In Proceedings of the world congress on engineering and computer science (Vol. 2, pp. 20-22).

[2] Plessky, V. P., & Reindl, L. M. (2010). Review on SAW RFID tags. IEEE transactions on ultrasonics, ferroelectrics, and frequency control, 57(3).

[3] Lazaro, A., Ramos, A., Girbau, D., & Villarino, R. (2011). Chipless UWB RFID tag detection using continuous wavelet transform. IEEE Antennas and Wireless Propagation Letters, 10, 520-523.

[4] Motakabber, S. M. A., Ibrahimy, M. I., & Alam, A. Z. (2013, August). Development of a position detection technique for UWB chipless RFID tagged object. In Computing, Electrical and Electronics Engineering (ICCEEE), 2013 International Conference on (pp. 735-738). IEEE.

[5] Zheng, Li-Rong, Meigen Shen, Xingzhong Duo, and Hannu Tenhunen. "Embedded smart systems for intelligent paper and packaging." In Electronic Components and Technology Conference, 2005. Proceedings. 55th, pp. 1776-1782. IEEE, 2005.

[6] Chamarti, A., & Varahramyan, K. (2006). Transmission delay line based ID generation circuit for RFID applications. IEEE microwave and wireless components letters, 16(11), 588-590.

[7] Shao, B., Chen, Q., Amin, Y., David, S. M., Liu, R., & Zheng, L. R. (2010, November). An ultra-low-cost RFID tag with 1.67 Gbps data rate by ink-jet printing on paper substrate. In Solid State Circuits Conference (A-SSCC), 2010 IEEE Asian (pp. 1-4). IEEE.

[8] Preradovic, S., Balbin, I., Karmakar, N. C., & Swiegers, G. F. (2009). Multiresonator-based chipless RFID system for low-cost item tracking. IEEE Transactions on Microwave Theory and Techniques, 57(5), 1411-1419.

[9] Motakabber, S. M. A., Ibrahimy, M. I., & Hossain, A. K. M. (2017). Generating an energy efficient discrete chirp signal for UWB chipless RFID reader circuit. IRAJ Reserach Forum, Institute of Reserach Journal.

[10] D.M. Pozer, Microwave Engineering, 4th Edition, Wiley, New York, 1998.

[11] CST, CST Microwave Studio, user manual, 2013.